Winter 2024

Engineering Mussel Foot Protein 5 (MFP5) for Enhanced Adhesive Performance in Tendon and Bone Repair

Ziyue Zhu
Washington University – McKelvey School of Engineering

WASHINGTON UNIVERSITY IN ST. LOUIS

McKelvey School of Engineering
Department of Biomedical Engineering

Thesis Examination Committee:
Fuzhong Zhang, Chair
Dennis Barbour
Michael Vahey

Engineering Mussel Foot Protein 5 (MFP5) for Enhanced Adhesive Performance in Tendon and Bone Repair

by

Ziyue Zhu

A thesis presented to
the McKelvey School of Engineering
of Washington University in
partial fulfillment of the
requirements for the degree
of Master of Science

December 2024
St. Louis, Missouri

Table of Contents

List of Figures

List of Tables

Acknowledgments

I sincerely thank my advisor, Prof. Fuzhong Zhang, for his invaluable advice, support, and guidance throughout my thesis research. His expertise and encouragement have been essential in completing this work. I am also immensely grateful to Kok Zhi Lee, who helped me significantly when I joined the lab. His patient instruction in protein purification and bacterial culture techniques laid a solid foundation for my research. Special thanks to Juya Jeon for her insightful suggestions and continuous support, which significantly contributed to the development and progress of my research. Lastly, I thank all my lab members and colleagues for their encouragement and assistance throughout this journey.

Ziyue Zhu

Washington University in St. Louis

December 2024

ABSTRACT OF THE THESIS

Engineering Mussel Foot Protein 5 (MFP5) for Enhanced Adhesive Performance in Tendon and Bone Repair

by

Ziyue Zhu

Master of Science in Biomedical Engineering

Washington University in St. Louis, 2024

Professor Fuzhong Zhang, Chair

This study explores the development of Mussel Foot Protein 5 (MFP5) bioadhesives to improve tendon-to-tendon and tendon-to-bone adhesive outcomes. MFP5, known for its underwater adhesive properties, was synthesized using recombinant techniques and optimized through coacervation and cross-linking. Adhesion tests demonstrated the superior performance of the optimized MFP5 adhesive on the tendon and bone samples. Improved protein concentration testing and purification methods enhanced MFP5 yield and consistency. Future research will focus on further standardization, exploring alternative purification methods, and evaluating the adhesive's performance in animal models. This study lays a foundation for developing robust MFP5-based bioadhesives, potentially revolutionizing surgical repair techniques and enhancing tissue integration and healing.

Chapter 1: Introduction

1.1 Importance of tissue adhesion in surgical procedures

Tissue adhesion plays a pivotal role in surgical procedures, facilitating the binding of tissue surfaces to accelerate healing and repair. This process is not just essential but transformative for restoring the function and integrity of damaged tissues, aiming to minimize post-operative complications such as infections and scarring and to enhance functional recovery. The advancement of tendon adhesion research is crucial, particularly for tendon-to-tendon and tendon-to-bone adhesions, where robust adhesion is necessary to withstand physiological stresses and ensure the functional integrity of repaired tissues [1]. Studies have shown that improved adhesion methods can significantly reduce recovery times and increase the success rates of surgical repairs, highlighting the importance of developing superior bioadhesives [19, 20].

1.2 Traditional sutures and their limitations

Traditionally, sutures have been the standard in managing tendon injuries, valued for their robust mechanical strength and versatility [2]. Sutures facilitate healing by strategically placing and securing surgical ties, which are vital in rejoining severed tendons and supporting the healing process [3]. Despite their effectiveness, the invasive nature of sutures, involving tissue penetration, can lead to additional trauma and adverse tissue reactions. These reactions can complicate recovery, potentially leading

to granµLomas that require surgical removal and may predispose the site to infections [4]. Given these challenges, there is a growing interest in alternative wound closure techniques that offer less invasive and more reliable solutions.

1.3 Advantages and limitations of medical adhesives

Medical adhesives, or bioadhesives, have emerged as indispensable tools in modern surgical procedures. These adhesives provide direct tissue adhesion at the application site, offering benefits such as reduced trauma, the elimination of sutures, superior cosmetic outcomes, and decreased pain compared to traditional suturing methods [5].

Despite their advantages, medical glues like cyanoacrylates, although fast-setting and strong, have been associated with significant foreign body reactions [6]. These reactions can lead to severe complications, duodenal perforation, colonic erosion and perforation, respiratory complications, etc. [7, 8], underscoring the need for innovative adhesive solutions with improved biocompatibility and mechanical properties.

1.4 Objectives and Potential Impact

This research focuses on developing a unique protein-based adhesive derived from natural sources specifically designed to form a scaffold structure at the tendon-to-tendon or tendon-to-bone interfaces. This innovative bioadhesive is intended to adhere

tissues effectively and support tissue integration and healing by providing a conducive environment for cellular growth. The unique properties of this adhesive, such as its biocompatibility and ability to degrade into non-toxic, naturally occurring amino acids, minimize the likelihood of adverse immune reactions, making it an ideal candidate for medical applications [9].

Furthermore, the project seeks to overcome the limitations of existing medical adhesives by enhancing mechanical properties and reducing the risk of foreign body reactions, thereby promising to improve recovery times and success rates of surgical repairs significantly. The successful development of this bioadhesive could revolutionize the field of surgical repair, particularly in complex tendon injuries, by providing a safer, more effective alternative to traditional suturing techniques.

Chapter 2: Background

2.1 Overview of MFP5 and its adhesive properties

Mussel Foot Protein 5 (MFP5) plays a crucial role in the byssal threads mussels use for secure adhesion in marine environments. This protein is an exemplary model for developing surgical adhesives that can operate effectively in moist conditions—an essential characteristic for medical applications, given the inherently wet physiological environments where such adhesives are employed. MFP5 is renowned for its robust adhesive capabilities, primarily due to its high levels of dihydroxyphenylalanine (DOPA) residues, contributing to its strong binding and durability [10]. Recent advances in synthetic biology and protein engineering have facilitated the recombinant production of MFP5, enabling precise control over its amino acid composition. This technological progress not only enhances the scalability of MFP5 production but also optimizes its adhesive properties for specialized medical applications [11]. By harnessing these innovations, MFP5-based adhesives can significantly improve surgical outcomes, offering a biocompatible and effective solution miming natural adhesion mechanisms.

2.2 Detailed explanation of the coacervation process

This study harnesses the coacervation method, a form of liquid-liquid phase separation, to enhance the underwater adhesive properties of MFP5. Coacervation effectively

segregates a homogeneous colloidal solution into two distinct phases: a denser, colloidal-rich phase known as the coacervate and a dilute phase with fewer colloidal components [13]. This separation concentrates the MFP5, making it more effective for underwater applications and preventing dilution in aquatic environments, ensuring that the adhesive maintains its integrity and does not wash away [14].

The coacervation process significantly protects and stabilizes MFP5's bioactive components from environmental factors, thus preserving their functional efficacy over time [12]. Concentrating on MFP5 creates a potent adhesive phase superior for robust underwater adhesion and overcoming the limitations commonly associated with conventional adhesives.

Coacervation promotes an environment that enhances the binding interactions of MFP5 with various surfaces, which is particularly beneficial given MFP5's natural propensity to form dense, cohesive phases in saline environments [15]. Using sodium dodecyl benzene sulfonate (SDBS), an anionic surfactant, further amplifies these properties. As illustrated in Figure 1(b), SDBS engages in electrostatic interactions with the positively charged amino acids in MFP5, such as lysine and arginine (Figure 1(a)), initiating coacervate formation. This interaction is bolstered by the arginine residues, which, due to their guanidine groups, facilitate strong cation-π and charge-charge interactions, contributing to the coacervate's stability and adhesive strength [16]. Moreover, the hydrophobic tail of SDBS interacts with MFP5’s non-polar sections, enhancing the

durability and mechanical integrity of the coacervate.

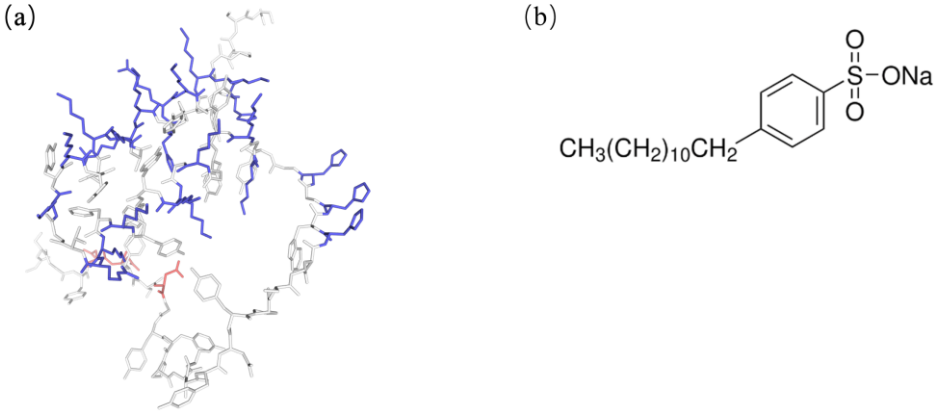

Figure 1. (a) The 3D Structure of MFP5. This diagram showcases the intricate molecular structure of MFP5, highlighting the key residues critical for its functionality as an underwater bioadhesive. The blue regions represent lysine residues, and the red regions denote arginine residues, both pivotal for the protein's interactions and adhesive capabilities. These essential amino acids facilitate electrostatic interactions with negatively charged molecules. (b) Structure of SDBS. The structure features a benzene ring attached to a sulfonyl group, which imparts a negative charge. The long hydrophobic tail, consisting of a 12-carbon alkyl chain, enhances its compatibility with non-polar substances, effectively reducing surface tension and stabilizing emulsions by forming micelles in aqueous solutions.

2.3 Importance of crosslinking in enhancing adhesive performance

A good bioadhesive requires both cohesion and adhesion. To make the bioadhesive more cohesive and stable, crosslinking is applied to the MFP5 coacervate. This process

enhances the adhesive's thermal stability and environmental stress resistance, ensuring it retains its cohesive strength and durability in challenging underwater conditions [17].

Collagen, a vital natural biopolymer, is a primary component of both tendons and bones, forming over 80% of the dry weight of tendons [18, 21]. Given its significant structural role, enhancing collagen's properties through crosslinking is crucial for maintaining the integrity and functionality of these tissues.

Glutaraldehyde (GA), a five-carbon molecµLe with aldehyde groups at both ends, stands out as a preferred crosslinking agent due to its ability to improve the mechanical properties of collagen-based materials [18]. Figure 2 illustrates the chemical interaction between GA and collagen, depicting the crosslinking process that enhances the biomechanical properties of the collagenous matrix [18]. The left side of the diagram shows the individual structures of GA and collagen, while the right side displays the Resultant GA-collagen crosslink.

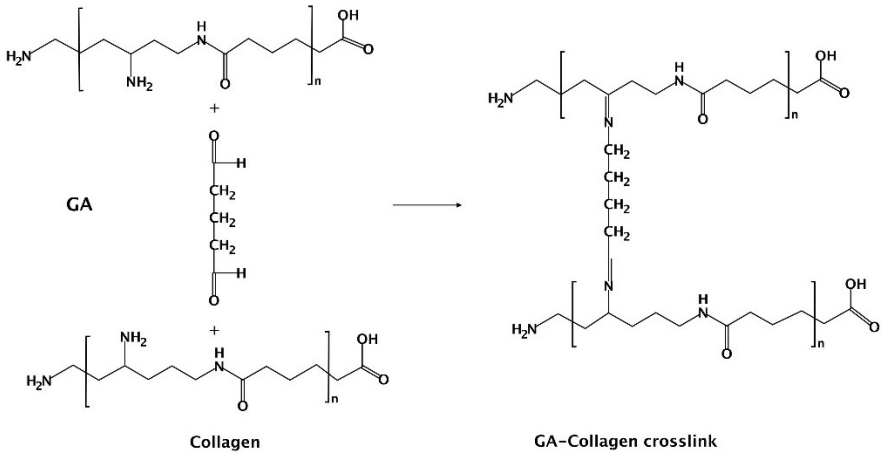

Figure 2. Chemical interaction between GA and collagen, depicting the crosslinking

process that enhances the biomechanical properties of the collagenous matrix [18].

GA is commonly used as a cross-linking agent in producing biomedical items such as heart valves, vascμLar grafts, elastic cartilages, tendon xenografts, and artificial skin [18]. Given its widespread use in crosslinking biomaterials, GA is ideally suited for crosslinking MFP5 coacervates. This process forms a solid network, potentially allowing cells to grow into it and crosslinks the MFP5 coacervates to tissues such as tendons and bones. There are two types of crosslinks: one type involves the reaction between the ε-amine groups found in lysine residues of MFP5 and the aldehyde groups of GA, where both aldehyde groups of GA interact with lysine residues in MFP5, forming a solid network conducive to cellμLar growth. The other type of crosslink is formed through the reaction of one aldehyde group of GA with the ε-amine groups of lysine or hydroxylysine residues in collagen. In contrast, the other aldehyde group reacts with lysine residues in the MFP5 coacervate. This dual interaction crosslinks the MFP5 networks with the injury interface (tendons and bones), thereby aμgmenting its adhesive and cohesive ability.

Chapter 3: Methods

3.1 Chemicals and Reagents

All chemicals and reagents, unless otherwise noted, were sourced from Sigma-Aldrich (St. Louis, MO). For plasmid cloning, gel extraction kits and plasmid miniprep kits from iNtRON Biotechnology (SeoμL, Republic of Korea) were utilized according to the respective manufacturer's protocols. Phusion DNA polymerase, FastDigest restriction enzymes, and T4 DNA ligase from Thermo Fisher Scientific (MA) were used for all PCR, digestion, and ligation procedures following the provided guidelines. Ni-NTA columns employed in this study were procured from Cytiva (Marlborough, MA).

3.2 Plasmid Construction

The construction of the plasmid for MFP5(1) was carried out by Eμgene et al. (2018) using a BioBrick system, depicted in Figure 3(a). This system was employed to express MFP5(1) and included an AKTK expression tag and an H6 purification tag. Key elements incorporated in this system are ribosome binding sites (RBS), 5′-untranslated regions (5′-UTR), antibiotic resistance markers, promoters, origins of replication, and restriction sites, which are schematically represented in Figure 3.

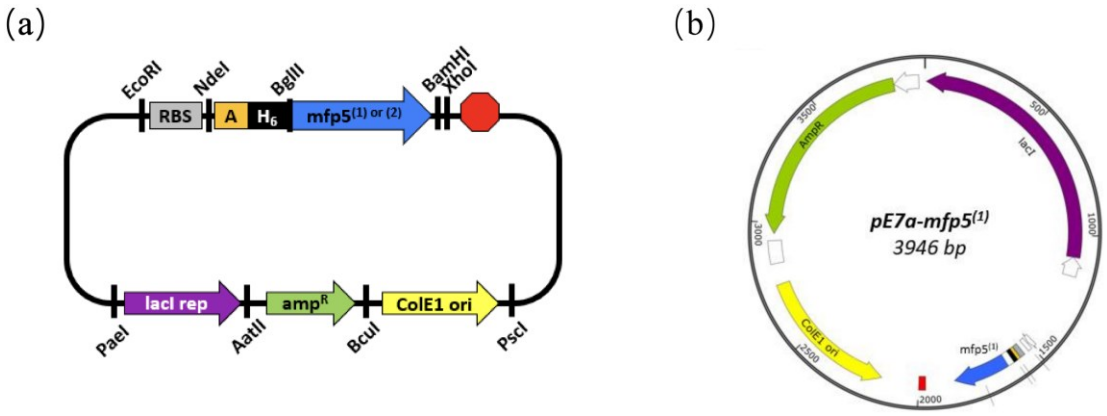

Figure 3. (a) BioBricks assembly system. It is used for expressing MFP5(1), along with an AKTK expression tag and an H6 purification tag. (b) Plasmid maps for pE7a-MFP5 [10].

This study used the E. coli strain MDS42pdu as the host for cloning all genes and plasmids. The MFP5 amino acid sequence was optimized for E. coli expression utilizing the Gene Designer 2.0 software from DNA 2.0 Inc. Integrated DNA Technologies Inc. (San Jose, CA) chemically synthesized the optimized DNA sequences and subsequently amplified them using polymerase chain reaction (PCR) with specific forward and reverse primers. The sequences are provided in Table 1.

Name	Sequence	Description
mfp5(1)	GCTAAGACTAAA**CATCATCACCATCACCAC**GGTGGCGGTGGCAG CAGATCTGGATCTAGCAGCGAAGAGTATAAAGGTGGTTACTACCC GGGCAACACTTACCACTACCATAGCGGCGGCTCCTACCACGGTTCC GGCTATCACGGTGGCTACAAAGGTAAATACTACGGCAAAGCGAAA AAGTACTACTACAAATATAAAAACTCCGGCAAATACAAGTATCTG AAGAAGGCTCGTAAATATCACCGTAAAGGTTACAAAAAGTATTAC GGCGGTGGTTCTTCTGGATCC	The coding sequence for the Mfp5(1) includes sequences for the AKTK expression tag, the **His6 affinity tag**, as well as linker and BioBrick cut sites. This design and construction were detailed by Eugene et al. (2018).
BglII-Mfp5-F	AAAAAAAGATCTAGCAGCGAAGAGTATAAAGGTG	A forward primer was designed for the amplification of the mfp5 gene, incorporating a BglII overhang to facilitate its insertion into the pE7a-AKTK-H6 backbone, as described by Eugene et al. (2018).
BglII-Mfp5-R	AAAAAAGGATCCAGAAGAACCACCGCCG	A reverse primer was designed for the amplification of the mfp5 gene, including a BamHI overhang to enable its insertion into the pE7a-AKTK-H6 backbone, as reported by Eugene et al. (2018).

Table 1. Coding sequences of MFP5, forward and reverse primer.

To facilitate insertion into the pE7a-AKTK-H6 backbone, the MFP5(1) genes were amplified with BglII and BamHI sites on the 5′ and 3′ ends, respectively [10]. Both the amplified gene and the backbone were digested with BglII and BamHI. The backbone was treated with alkaline phosphatase to prevent unwanted recircμLarization. The digested backbone and gene inserts were ligated using T4 ligase. The correct orientation of each gene within the isolated plasmid was verified through restriction digestion with BglII and BamHI, followed by Sanger sequencing conducted by Eurofins Genomics (Louisville, KY).

3.3 Expression of Recombinant Proteins

3.3.1 Transformation and Culture

E. coli strain BL21(DE3) (Thermo Fisher Scientific, Waltham, MA) was used as the

host for expressing MFP5. The plasmid containing the MFP5 gene was transformed into E. coli via electroporation using an Eporator (Eppendorf, Hamburg, Germany). For electroporation, 100 µL of E. coli strain BL21(DE3) at a concentration of approximately 10^9 cells/mL was mixed with 1 µL of plasmid DNA at 200 ng/µL. This mixture was placed in a 1 mm electroporation cuvette (Eppendorf, Hamburg, Germany). The Eporator settings were 1.8 kV, 25 µF, and 200 ohms. After electroporation, the solution was transferred into 1 mL of SOC (Super Optimal Broth with Catabolite Repression) medium, which contained 20 g/L tryptone, 5 g/L yeast extract, 0.5 g/L sodium chloride, 0.2 g/L potassium chloride, 2.46 g/L magnesium sµLfate, 2.03 g/L magnesium chloride, and 3.6 g/L glucose. The cells were incubated for 1 hour to recover.

3.3.2 Isolation and Initial Culture

Post-recovery, the cells were centrifuged, and the pellet was spread on Luria-Bertani (LB) agar plates, followed by incubation at 37°C for 16 hours to isolate colonies. Colonies containing the plasmid were Cultured in LB broth containing 10 g/L tryptone, 10 g/L sodium chloride, and 5 g/L yeast extract, supplemented with 100 µg/mL ampicillin. Freshly transformed colonies were grown in 5 mL of LB medium at 37°C for 5 hours and then transferred to 400 mL of LB medium for overnight Culture at 37°C.

3.3.3 Large-Scale Culture and Induction

The overnight Cultures were used to inocµLate 1 L of fresh LB medium in Erlenmeyer

flasks, starting at an initial OD600 of 0.08. The cultures were grown at 37°C and shaken until they reached an OD600 of 0.6. At this point, they were induced with 500 µM IPTG. Following induction, the cultures were further incubated at 37°C, shaking at 250 rpm for an additional 5–7 hours. Cells were harvested by centrifµgation at 4500g for 20 minutes at 4°C. The centrifuged cell pellets were either directly used for extraction or stored at -80°C until needed.

3.4 Protein Purification

For the purification of MFP5, cell pellets were resuspended in 10 mL of guanidine lysis buffer (6 M guanidine hydrochloride, 50 mM potassium phosphates, and 300 mM sodium chloride, pH 7.4) per gram of wet cells and lysed by agitation at 250 rpm. The lysates were centrifuged at 20,000g for 20 minutes at 18°C. To reduce viscosity, the collected lysates were sonicated on ice for 1.5 hours using a QSonica probe sonicator with 5-second on/off cycles. The lysates were then filtered through 0.2 µm filter membranes.

The proteins were purified using an AktaPure Fast Protein Liquid Chromatography (FPLC) system (GE Healthcare Inc., Chicago, IL) equipped with two 5 mL nickel affinity chromatography columns (Cytiva, Marlborough, MA). The columns were pre-equilibrated with guanidine lysis buffer prior to sample loading. After loading, the columns were washed with 5–10 column volumes (CVs) of guanidine wash buffer (6

M guanidine hydrochloride, 50 mM potassium phosphates, 300 mM sodium chloride, and 25 mM imidazole, pH 7.4). The proteins were eluted and fractionated using 5–10 CVs of guanidine elution buffer (6 M guanidine hydrochloride, 50 mM potassium phosphates, 300 mM sodium chloride, and 250 mM imidazole, pH 7.4).

SDS-PAGE analyzed purified MFP5 proteins, which were dialyzed at 4°C using 2.5% acetic acid and 3500 MWCO SnakeSkin™ Dialysis Tubing (Thermo Fisher Scientific, Waltham, MA), with buffer changes twice a day for three days. The purified MFP5 proteins were subsequently lyophilized using FreeZone 4.5 Liter -84°C Benchtop Freeze Dryers (Labconco Corporation, Kansas City, MO) for five days and then stored at -20°C for future use.

3.5 SDS-PAGE

Sodium dodecyl sµLfate-polyacrylamide gel electrophoresis (SDS-PAGE) was performed using 1 mm-thick gel cast in Bio-Rad casting cases (Bio-Rad, HercµLes, CA). The gels consisted of a 14% polyacrylamide separating gel (containing 14% bisacrylamide, 375 mM Tris at pH 8.8, 0.1% SDS, 0.1% ammonium persµLfate (APS), and 0.04% tetramethylethylenediamine (TEMED)) and a 5% polyacrylamide stacking gel (comprising 5% bisacrylamide, 125 mM Tris at pH 6.8, 0.1% SDS, 0.1% APS, and 0.1% TEMED). Purified protein samples were loaded into the gel lanes.

The electrophoresis was conducted using Mini-PROTEAN Tetra Cells (Bio-Rad) in 1× TGS buffer (30 g/L Tris, 144 g/L glycine, and 10 g/L SDS) at a voltage of 145 V for 120 minutes or until the dye front exited the gel. Following electrophoresis, gels were stained with Coomassie Blue staining solution (40% methanol, 7% acetic acid, and 0.1% Coomassie Brilliant Blue) for 60 minutes at room temperature with gentle agitation. The gels were then destained in a solution containing 40% methanol and 7% acetic acid for at least 60 minutes before being imaged using an Azure c600 Imager (Azure Biosystems, Dublin, CA).

3.6 Protein Concentration Testing

Protein concentration was determined using two methods: the Quick Start™ Bradford Protein Assay (Bio-Rad, HercµLes, CA) and the Nanodrop 2000c spectrophotometer (Thermo Fisher Scientific, Waltham, MA). The Bradford assay was performed according to the manufacturer's instructions, providing a colorimetric method to quantify protein levels. Additionally, the Nanodrop 2000c was utilized for its ability to measure absorbance directly, offering a rapid and accurate assessment of protein concentration.

3.7 MFP5 adhesive preparation

3.7.1 Coacervation

To prepare the coacervation, 20 mg of lyophilized MFP5 protein was resuspended in 100 mM sodium acetate buffer at pH 5.5. The protein solution concentration was adjusted to 1 µg/µL. SDBS was separated in the same sodium acetate buffer to a 36 µg/µL concentration. The coacervation process required a ratio of 2 µg of SDBS per 1 µg of MFP5 protein. After mixing the required amount of SDBS with the resuspended MFP5 protein solution, the tube was inverted gently for 10 seconds to facilitate coacervation, indicated by the solution turning turbid (Figure 4(a)). The turbid mixture was then centrifuged at 15,000 rpm for 5 minutes, and the supernatant was discarded, leaving a concentrated MFP5 protein pellet awaiting crosslinking (Figure 4(b)).

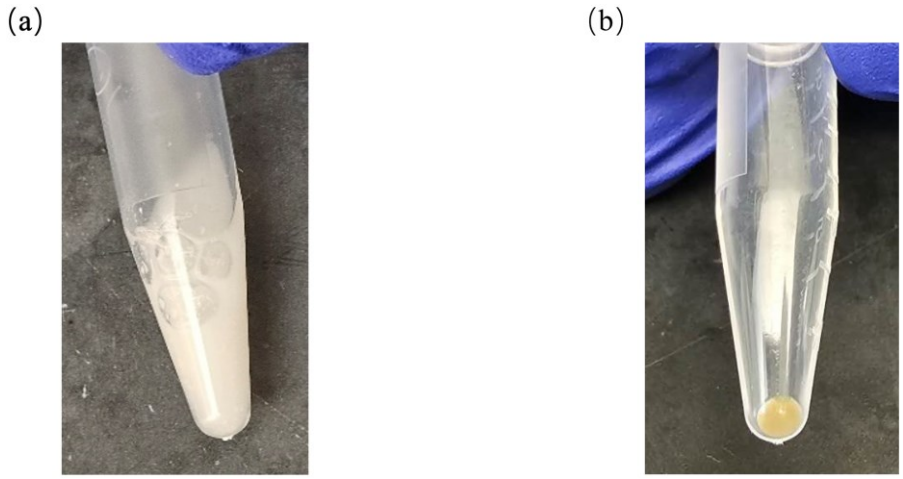

Figure 4. (a) The turbid solution indicating the coacervation of MFP5 protein after the addition of SDBS. (b) The concentrated MFP5 protein pellet was obtained after centrifµgation and removal of the supernatant.

3.7.2 Crosslinking

A 250 µL of 0.25% glutaraldehyde (GA) solution was added to the tube containing the

MFP5 protein pellet, and the mixture was incubated on ice for 25 minutes. Following incubation, the supernatant was discarded, and the pellet was washed with 500 μL of 100 mM sodium acetate buffer. At this stage, the MFP5 bioadhesive was prepared and ready for adhesion testing.

3.8 Sample preparation

Bovine tendons and bones were obtained from a local butcher in St. Louis for this study. The tendons were initially sectioned into cuboids measuring 4 cm by 1.5 cm. The microtome (Thermo Fisher Scientific, Waltham, MA) was set to -20°C to facilitate precise slicing. Each 4 cm by 1.5 cm tendon cuboid was embedded in Tissue-Tek® O.C.T. Compound (Sakura Finetek USA, Torrance, CA) to provide support during sectioning. Once embedded, the tendon sections were cut to a uniform thickness of 1.5 mm using a microtome (Thermo Fisher Scientific, Waltham, MA). This ensured consistent sample size and surface smoothness for all tendon samples, which is critical for the reproducibility and accuracy of subsequent adhesion testing.

Bovine bones were prepared using a precision circular saw to cut cuboids of identical dimensions, 4 cm by 1.5 cm, with a thickness of 1.5 mm. This careful preparation ensured that the mating surfaces for adhesive testing were flat and uniform, essential for the reliability of shear strength measurements.

After preparation, tendon and bone samples were stored at -20°C in airtight containers to prevent dehydration and degradation. Before adhesive application, the samples were gradually thawed to room temperature to closely mimic physiological conditions.

3.9 MFP5 Adhesive Application

The MFP5 adhesive was uniformly applied at the interface between the prepared tendon and tendon/bone samples. To ensure consistency, the volume of MFP5 adhesive used in each test was standardized to 5 mm x 5 mm x 1 mm. After applying the MFP5 adhesive between the samples, a 1 kg weight was evenly placed on top of the cross-sectional area to ensure consistent adhesive contact during curing.

The samples with the weight were submerged in a bowl of deionized (DI) water throughout the curing period to maintain hydration and simulate physiological conditions. The adhesive was allowed to cure at 37°C for 16 hours to ensure optimal bonding strength. This controlled environment ensured uniform curing and consistent results across all samples.

3.10 Underwater Adhesion Testing

The lap shear strength of the bonded samples was measured using an MTS Criterion Model 41 universal test frame fitted with a 25 N load cell (MTS Systems Corporation,

Eden Prairie, MN). Each sample assembly was mounted on the tensometer such that the tensile load was applied parallel to the plane of the adhesive bond. The test was conducted at a crosshead speed of 2 mm/min until bond failure occurred.

The peak load at failure was recorded, and the shear strength was calculated by dividing the peak load by the overlapped area, which was measured using ImageJ software. The adhesion strength (P) in pascals was calculated using the equation: $P = \frac{F}{A}$, where F is the peak load, and A is the final area of the MFP5 adhesive at the point where the MTS machine pulled apart the two samples. This method ensures precise measurement of the adhesive strength under standardized testing conditions.

3.11 ImageJ Setup

After the adhesion tests, the area of the MFP5 adhesive was determined using ImageJ software (National Institutes of Health, Bethesda, MD). A ruler was placed near the MFP5 adhesive sample to measure the adhesive area accurately, and a photograph was taken. The image was then imported into ImageJ for analysis. The scale was set using the ruler in the image to ensure accurate measurement, which was achieved by selecting a known length on the ruler and setting the scale in ImageJ accordingly. The adhesive area was outlined using the freehand selection tool to capture the irregular shape of the adhesive precisely. Once the area was selected, the 'Measure' function calculated the area in square millimeters. This method ensured precise and reproducible measurement

of the adhesive area, which is critical for accurately calculating adhesion strength.

Chapter 4: Results and Conclusion

A series of tests using various concentrations of GA was conducted to identify the optimal concentration of GA for crosslinking the MFP5 pallet after coacervation. The objective was to evaluate the lap shear strength of the adhesive bonds formed between tendon and tendon samples at different GA concentrations.

Figure 5 demonstrates a non-linear relationship between GA concentration and lap shear pressure, indicating that there is an optimal concentration of GA for maximizing adhesive strength. For each concentration, three replicate tests were conducted to ensure the reliability and accuracy of the results. The data points form a bell-shaped curve, suggesting that 0.25% GA is the optimal concentration for achieving the highest adhesive strength. This bell-shaped curve highlights the importance of optimizing GA concentration, as both insufficient and excessive crosslinking can negatively impact the adhesive performance.

At 0.00% GA concentration, the lap shear pressure is at its lowest, which is reasonable due to no crosslinking process is involved. As the GA concentration increases to 0.10%, the lap shear pressure rises significantly to around 600 kPa. This indicates an improvement in adhesive strength due to the initiation of crosslinking. The lap shear pressure peaks at approximately 1500 kPa at a GA concentration of 0.25%. This peak suggests that 0.25% GA provides the optimal level of crosslinking, enhancing the

adhesive strength to its maximum.

Beyond 0.25%, the lap shear pressure starts to decline. At 0.50% GA, the pressure drops to around 900 kPa. This decrease may be due to over-crosslinking, which can make the adhesive too rigid and less effective. At 1.00% GA, the lap shear pressure further decreases to approximately 500 kPa, indicating a continued decline in adhesive performance. The lowest point on the graph after the initial rise is at 2.00% GA, where the lap shear pressure drops back to around 200 kPa. This suggests that excessive GA concentration can significantly reduce the adhesive strength, likely due to the formation of a brittle and over-crosslinked network.

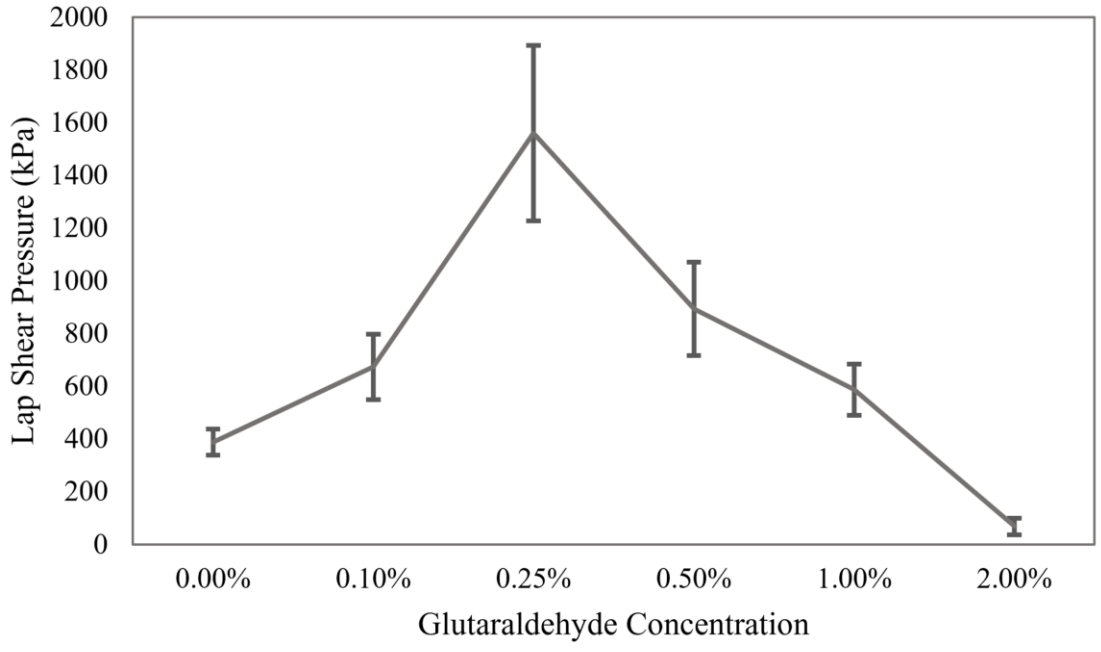

Figure 5. The relationship between glutaraldehyde (GA) concentration and lap shear pressure. The highest adhesive strength is observed at 0.25% GA concentration with a peak lap shear pressure of approximately 1800 kPa. Error bars indicate the standard

deviation from three replicate tests per concentration.

The relationship between the MFP5 and SDBS ratios was evaluated to determine their effects on the size and mechanical properties of the adhesive. As shown in Figure 6(a), different MFP5/SDBS ratios (2.88:1, 2.5:1, 2.25:1, and 2:1) resulted in significant differences. Under the same batch and concentration of MFP5, higher SDBS levels led to a smaller and more translucent MFP5 adhesive.

Conversely, using an excess amount of MFP5 while maintaining a constant SDBS level, such as in a 3.5:1 ratio, caused visible aggregation (yellow spots) immediately after mixing, as shown in Figure 6(c). In contrast, an optimal MFP5 ratio produced a turbid yet clear solution without visible aggregation, as illustrated in Figure 4(a).

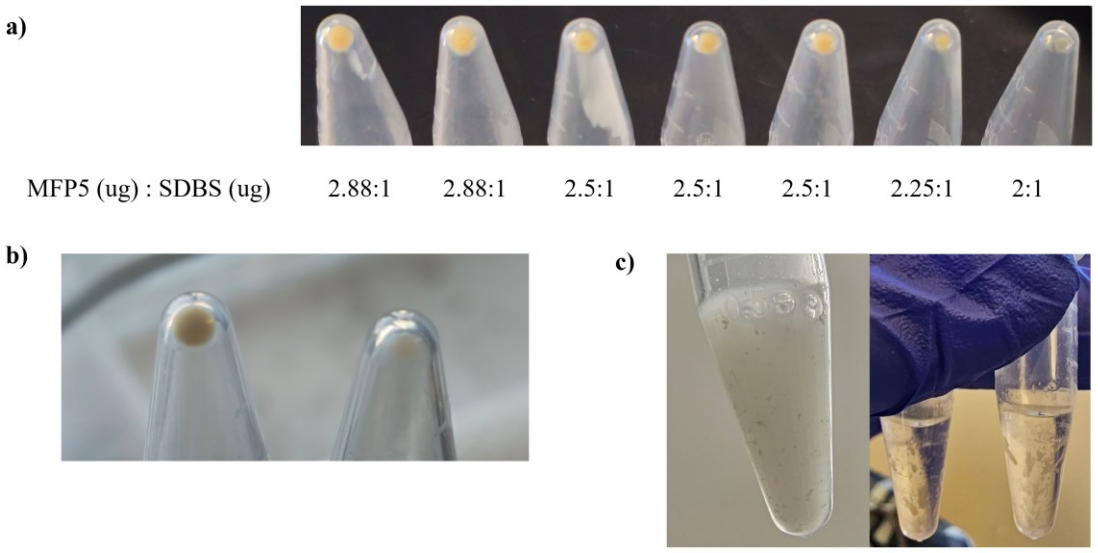

Figure 6. (a) Effects of different MFP5/SDBS ratios on the size and translucency of the MFP5 adhesive. Ratios tested include 2.88:1, 2.5:1, 2.25:1, and 2:1. (b) Close-up

comparison of MFP5/SDBS ratios of 3:1 vs. 2:1. (c) Left: Visible aggregation observed at a 3.5:1 MFP5 ratio. Right: After centrifugation, the coacervate sticks to the tube wall, making it difficult to collect.

As the physical appearance of the MFP5 adhesive changes with varying MFP5 ratios, it was essential to evaluate if these ratios also influence the adhesive properties. Figure 7 illustrates the lap shear pressure results when applying MFP5 adhesive between tendon and bone samples for three different MFP5/SDBS ratios. For each ratio, three replicate tests were conducted to ensure the reliability and accuracy of the results. Although the performance differences among these ratios are not dramatic, the 2:1 ratio stands out, achieving approximately 750 kPa of lap shear pressure. This indicates that the 2:1 ratio provides the optimal balance between MFP5 and SDBS for maximum adhesive strength, despite the other ratios showing slightly lower performance.

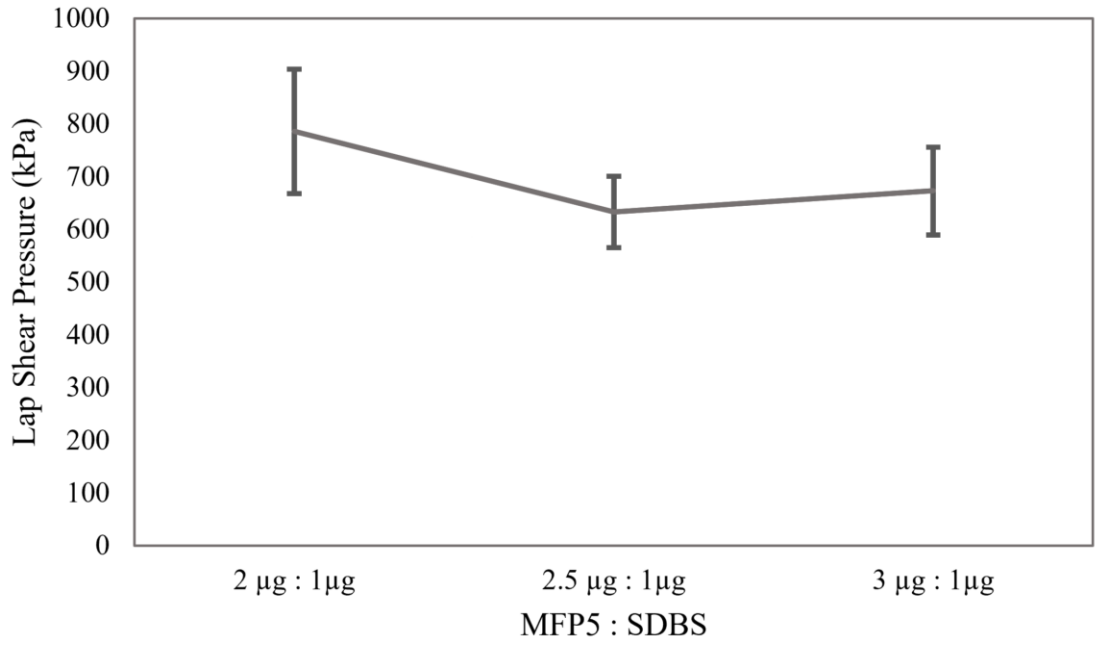

Figure 7. The relationship between different MFP5/SDBS ratios and the resulting lap shear pressure (kPa).

In conclusion, the optimal MFP5: SDBS ratio for coacervation is 2 µg: 1µg, and the optimal GA concentration for crosslinking is 0.25%. These findings highlight the critical importance of precise formulation in developing effective MFP5 bioadhesives. A robust and reliable adhesive suitable for both tendon-to-tendon and tendon-to-bone repair can be developed by standardizing each reaction condition. This research lays a strong foundation for further exploration and advancement of bioadhesive technologies, paving the way for improved medical applications and enhanced tissue repair strategies.

Chapter 5: Discussion

5.1 Low MFP5 yield

One of the primary challenges encountered in this research is the low yield of MFP5, which significantly restricts the number of tests conducted per bacterial culture cycle. From a 10-liter batch of LB medium, only approximately 200 mg of MFP5 is obtained, and each adhesion test requires around 40 mg of MFP5. Additionally, MFP5 does not fully dissolve in sodium acetate, necessitating only the supernatant from the resuspended MFP5 solution for these studies.

SDS-PAGE analysis was employed to investigate the underlying issues in protein yield, as depicted in Figure 8 a. All samples analyzed were collected from the flow-through of the HisTrap column. The samples were washed with 2 M Urea using Vivaspin 2 MWCO 3000 (Cytiva, Marlborough, MA) to exchange the imidazole in the wash buffer. This step ensures the proteins are adequately prepared for accurate analysis, minimizing potential artifacts or misinterpretations caused by imidazole.

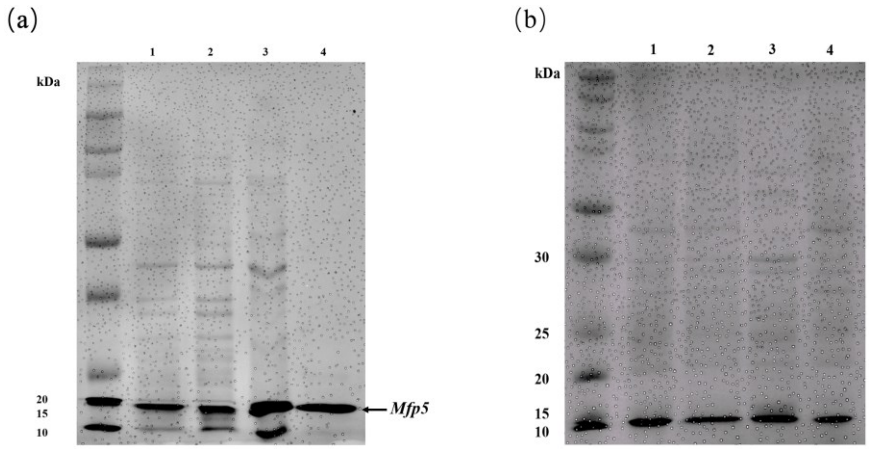

Figure 8. The SDS-PAGE gel shows the different stages of the purification process. (a) The lysate lane (lane 1) indicates the total protein content before purification. The flow-through lane (lane 2) shows proteins that did not bind to the column, including MFP5. The wash lane (lane 3) indicates proteins washed away during the purification process, and the elute lane (lane 4) shows the final purified MFP5 protein. (b) Re-purified MFP5 from the collected flow-through and wash fractions, demonstrating enhanced yield.

The SDS-PAGE results demonstrate MFP5 loss during the flow-through of the E. coli lysate through the purification column, indicating that the column has a low affinity towards MFP5. Additionally, MFP5 was washed away during the washing step, suggesting that the imidazole concentration in the wash buffer might be too high for MFP5.

To determine if the MFP5 that was washed away could be collected and re-purified, all the flow-through from lane 2 (flow-through) and lane 3 (wash) in Figure 8(a) were collected and subjected to re-purification. The sample from lane 3 in Figure 8(a) was treated with guanidine hydrochloride using Vivaspin 2 MWCO 3000 (Cytiva,

Marlborough, MA) to remove the imidazole. This re-purification explored whether recovering MFP5 from the wash could effectively minimize protein loss and enhance yield. As depicted in Figure 8(b), MFP5 was successfully purified from the collected flow-through, indicating the potential viability of this approach.

To optimize the purification protocol further, a third round of purification was conducted to determine the optimal imidazole concentration in the wash buffer. As demonstrated in Figure 9, MFP5 protein remained abundant in the flow-through even after this third purification attempt. An SDS-PAGE analysis was performed to identify potential protein loss during the imidazole/guanidine exchange process.

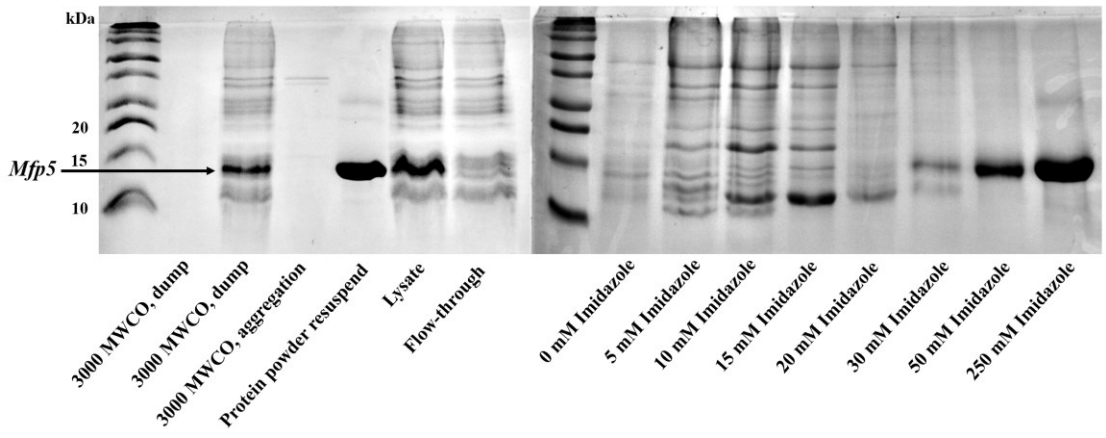

Figure 9. SDS-PAGE gel analysis of the third round of purification to determine the optimal imidazole concentration in the wash buffer. The results highlight the challenges in optimizing the purification protocol for MFP5 and suggest the necessity for an improved method to enhance the yield and purity of the target protein.

The results indicated that MFP5, despite having a molecular weight higher than the

3000 MWCO filter used, still showed presence in the bands on the gel. This suggests potential protein loss, possibly because MFP5, being a non-spherical protein, may be able to pass through the filter. These findings highlight several critical points.

Firstly, the HisTrap column exhibited a low affinity for MFP5, allowing the protein to be eluted at relatively low imidazole concentrations. The optimal imidazole concentration for MFP5 elution was identified as 30 mM. Secondly, due to the HisTrap column's low affinity for MFP5, multiple rounds of purification and chemical exchanges were necessary to achieve a satisfactory yield. Thirdly, during the process of collecting and storing the flow-through, there is a potential for MFP5 to degrade due to the multiple steps involved in the protein purification process.

In conclusion, while the HisTrap column can be used to purify MFP5, its low affinity necessitates extensive processing to achieve optimal yields. Although continuously collecting the flow-through and re-purifying it can enhance MFP5 yield, this approach is time-consuming and can lead to MFP5 degradation during the process. Identifying an alternative protein purification platform with a higher affinity for MFP5 would maximize yield and streamline the purification process, making it more efficient and reliable.

5.2 Protein concentration testing methods and SDBS/MFP5 ratio

The protein concentration testing methods are critical in this research because the MFP5/SDBS ratio significantly affects the coacervation process. Ideally, the protein concentration would be determined by weighing the lyophilized MFP5 and calculating the concentration. However, lyophilized MFP5 does not fully dissolve in water, complicating this approach. Initially, the Bradford assay was used to measure the MFP5 concentration. In the early stages, the data were stable, and the coacervation process was consistent. However, after a few months, the results became inconsistent, potentially due to contamination of the Bradford reagent. This inconsistency highlighted the need for a reliable protein concentration testing method. The accuracy of the MFP5 concentration is less critical than the consistency of the results when considering coacervation. A consistent protein concentration testing method is essential to maintain a consistent MFP5/SDBS ratio. Standardizing this ratio ensures that the coacervation process can be replicated reliably, thus providing stable and reliable data. Additionally, exploring alternative solvents or buffer systems more compatible with MFP5's chemical nature might be beneficial.

5.3 Sample preparation

The MFP5 adhesive performs optimally on a flat surface. While a flat surface can be achieved through microtoming tendon samples, bone surfaces are naturally rounded

and cannot be processed through a microtome, requiring manual modification to achieve a suitable surface for adhesive application. To maintain consistency in underwater adhesion tests, it is crucial to flatten the bone surface. However, modifying the bone surface may compromise its integrity by exposing the compact bone, which can potentially affect the consistency of the lap shear data. The research aims to design an MFP5 adhesive that can effectively adhere to the periosteum of the bone and tendon. Exposing the compact bone might introduce variability in the lap shear results. An ideal lap shear setup should ensure both surfaces are flat to provide reliable and consistent data (Figure 10).

Figure 10. Prepared tendon and bone samples used for adhesion testing with MFP5 adhesive. On the left, the bone sample has been modified to flatten its naturally rounded surface. On the right, the tendon sample has been microtomed into a flat surface, and the brown material is the MFP5 adhesive.

5.4 Future work

Given the complexity of the experiments in this research, standardizing experimental

conditions should be a primary focus for future studies. Optimal experimental conditions were determined progressively, initially leading to large error bars in the data. As the conditions became more standardized, the results became more reliable. Meticulous control of every aspect of the experiment is essential, as even minor variations can dramatically affect the data. Future work should refine these conditions further to ensure consistency and repeatability.

Additionally, exploring alternative methods and materials that could enhance the yield and performance of the MFP5 adhesive will be crucial. Continuous improvement in these areas will contribute to developing a robust and reliable bioadhesive for medical applications.

Once consistent results are achieved with tissue samples, evaluating the MFP5 adhesive in animal models will be necessary. This will help determine whether the material forms a scaffold structure that allows cell ingrowth and assess its adhesive performance in a living system. Furthermore, evaluating the material's ability to promote wound healing and recovery in animal models will provide valuable insights into its potential clinical applications.

References

1. Yang, Z., Ma, Z., Liu, S., Li, J. (2021). Tissue adhesion with tough hydrogels: Experiments and modeling. *Mechanics of Materials*, 157, 103800. ISSN 0167-6636. https://doi.org/10.1016/j.mechmat.2021.103800.

2. Rawson, S., Cartmell, S., Wong, J. (2013). Suture techniques for tendon repair; a comparative review. *Muscles Ligaments Tendons J.*, 3(3), 220-8. PMID: 24367784; PMCID: PMC3838333.

3. Bal-Ozturk, A., Cecen, B., Avci-Adali, M., Topkaya, S.N., Alarcin, E., Yasayan, G., Ethan, Y.C., Bulkurcuoglu, B., Akpek, A., Avci, H., Shi, K., Shin, S.R., Hassan, S. (2021). Tissue Adhesives: From Research to Clinical Translation. *Nano Today*, 36, 101049. doi: 10.1016/j.nantod.2020.101049. PMID: 33425002; PMCID: PMC7793024.

4. Arner, M., Unge, L., Franko, M.A., Svingen, J. (2023). Inflammatory reaction to suture materials after flexor tendon repair. A retrospective study of 594 patients. *Case Reports Plast Surg Hand Surg.*, 10(1), 2222807. doi: 10.1080/23320885.2023.2222807. PMID: 37351525; PMCID: PMC10283439.

5. Sunjic Roguljic, V., Roguljic, L., Kovacic, V., Jukic, I. (2023). A Comparison of Tissue Adhesive Material and Suture as Wound-Closure Techniques following Carpal Tunnel Decompression: A Single-Center Randomized Control Trial. *J Clin Med.*, 12(8), 2864. doi: 10.3390/jcm12082864. PMID: 37109201; PMCID: PMC10145928.

6. Bala, M.M., Şahin, A.A., Boz, M., Durukan, Y., Fırat, T., Pakdil, M., Özturan, K.E. (2021). Effects of Cyanoacrylate in Rabbits with Induced Achilles Tendon Rupture. *Med Sci Monit.*, 27, e929709. doi: 10.12659/MSM.929709. PMID: 34483334; PMCID: PMC8434771.

7. Deng, J., Zeng, Z., Liao, Y., Zhong, H., Zhang, H. (2023). Cyanoacrylate glue foreign body after CT-guided localization of a pulmonary nodule during video-assisted thoracoscopic surgery: a case report. *BMC Pulm Med.*, 23(1), 24. doi: 10.1186/s12890-023-02321-x. PMID: 36653826; PMCID: PMC9847023.

8. Li, W., Xiao, M., Chen, Y. et al. (2019). Serious postoperative complications induced by medical glue: three case reports. *BMC Gastroenterol.*, 19, 224. https://doi.org/10.1186/s12876-019-1142-6.

9. Chu, S., Wang, A.L., Bhattacharya, A., Montclare, J.K. (2022). Protein Based Biomaterials for Therapeutic and Diagnostic Applications. *Prog Biomed Eng (Bristol).*, 4(1), 012003. doi: 10.1088/2516-1091/ac2841. Epub 2021 Oct 26. PMID: 34950852; PMCID: PMC8691744.

10. Kim, E., Dai, B., Qiao, J.B., Li, W., Fortner, J.D., Zhang, F. (2018). Microbially Synthesized Repeats of Mussel Foot Protein Display Enhanced Underwater Adhesion. *ACS Applied Materials and Interfaces*, 10(49), 43003-43012. https://doi.org/10.1021/acsami.8b14890.

11. Jeon, K., Lee, Z., Zhang, X. et al. (2023). Genetically Engineered Protein-Based Bioadhesives with Programmable Material Properties. *ACS Appl Mater Interfaces*, 15(49), 56786–56795. DOI:10.1021/acsami.3c12919.

12. Molik, S.P., Rakshit, A.K., Pan, A., Naskar, B. (2022). An Overview of Coacervates: The Special Disperse State of Amphiphilic and Polymeric Materials in Solution. *Colloids Interfaces*, 6, 45. https://doi.org/10.3390/colloids6030045.

13. Zhao, W., Wang, Y. (2017). Coacervation with surfactants: From single-chain surfactants to gemini surfactants. *Advances in Colloid and Interface Science*, 239, 199-212. ISSN 0001-8686. https://doi.org/10.1016/j.cis.2016.04.005.

14. Stewart, R.J., Wang, C.S., Shao, H. (2011). Complex coacervates as a foundation for synthetic underwater adhesives. *Advances in Colloid and Interface Science*, 167(1-2), 85-93. ISSN 0001-8686. https://doi.org/10.1016/j.cis.2010.10.009.

15. Huynh, T.P., Chen, Y., Bach-Gansmo, F.L., Dehli, J., Ibsen, V.N., Foss, M., Tvilum, A.S., Zelikin, A.N., Birkedal, H. (2023). Efficient Wet Adhesion through Mussel-Inspired Proto-Coacervates. *Adv. Mater. Interfaces*, 10, 2201491. https://doi.org/10.1002/admi.202201491.

16. Wang, Z., Gu, X., Li, B., Li, J., Wang, F., Sun, J., Zhang, H., Liu, K., Guo, W. (2022). Molecularly Engineered Protein Glues with Superior Adhesion Performance. *Adv. Mater.*, 34, 2204590. https://doi.org/10.1002/adma.202204590.

17. Muhoza, B., Xia, S., Zhang, X. (2019). Gelatin and high methyl pectin coacervates crosslinked with tannic acid: The characterization, rheological properties, and application for peppermint oil microencapsulation. *Food Hydrocolloids*, 97, 105174. ISSN 0268-005X. https://doi.org/10.1016/j.foodhyd.2019.105174.

18. Adamiak, K., Sionkowska, A. (2020). Current methods of collagen cross-linking: Review. *International Journal of Biological Macromolecules*, 161, 550-560. ISSN 0141-8130. https://doi.org/10.1016/j.ijbiomac.2020.06.075.

19. Freedman, B.R., Kuttler, A., Beckmann, N. et al. (2022). Enhanced tendon healing by a tough hydrogel with an adhesive side and high drug-loading capacity. *Nat. Biomed. Eng.*, 6, 1167–1179. https://doi.org/10.1038/s41551-021-00810-0.

20. Zhang, R. (2022). Application of Biomaterials in Tendon Injury Healing and Adhesion in Sports. *Journal of Healthcare Engineering*, 5087468, 9 pages. https://doi.org/10.1155/2022/5087468.

21. Buckley, M.R., Evans, E.B., Matuszewski, P.E., Chen, Y.L., Satchel, L.N., Elliott, D.M., Soslowsky, L.J., Dodge, G.R. (2013). Distributions of types I, II and III collagen by region in the human supraspinatus tendon. *Connect Tissue Res.*, 54(6), 374-9. doi: 10.3109/03008207.2013.847096. PMID: 24088220; PMCID: PMC6056177.